Flocking and reorientation transition in the q-state active Potts model

Matthieu Mangeat[1], Swarnajit Chatterjee[1,2], Raja Paul[2] and Heiko Rieger[1]

[1]Center for Biophysics & Department for Theoretical Physics,
Saarland University, 66123 Saarbrücken, Germany

[2]School of Mathematical & Computational Sciences,
Indian Association for the Cultivation of Science, 700032 Kolkata, India

Tuesday, 15th December 2020

LPT Seminar, Toulouse

Short CV

- 1991 : Born in Nancy (Meurthe-et-Moselle).
- .... - 2012 : Baccalauréat S + CPGE, Bayonne (Pays Basque).
- 2012 - 2015 : ENS Ulm (Paris)
  02-07/2014 : M1 Internship supervised by H. Rieger, Saarbrücken (Germany).
  01-03/2015 : M2 Internship supervised by F. Zamponi, LPTENS (Paris).
- 2015 - 2018 : PhD thesis supervised by D. S. Dean and T. Guérin, LOMA (Bordeaux).
- 2018 - ... : Postdoc in the group of H. Rieger, Saarbrücken (Germany).
- 2021 : Candidate for the entrance to the CNRS.

Bystander cells enhance NK cytotoxic efficiency by reducing search time

- NK cytotoxic search infected cells, and meet bystander cells favourings their migration.
- We have studied a numerical model to understand these observations.
- The search time is reduced with the number of bystanders, and the interaction radius.

X. Zhou, R. Zhao, K. Schwarz, M. Mangeat, E. C. Schwarz, M. Hamed, I. Bogeski, V. Helms, H. Rieger, and B. Qu, Sci. Rep **7**, 44357 (2017).

Quantitative approximation schemes for glasses

- The glass transition depends on the kinetic of the cooling (not unique T_g).
- We have calculated the equation of state expanding its exact solution at $d = \infty$.
- We have constructed the phase diagram for all dimension $d \geq 3$ (correct for $d = 3$).

M. Mangeat and F. Zamponi, Phys. Rev. E **93**, 012609 (2016).

Dispersion in complex media (1/2)

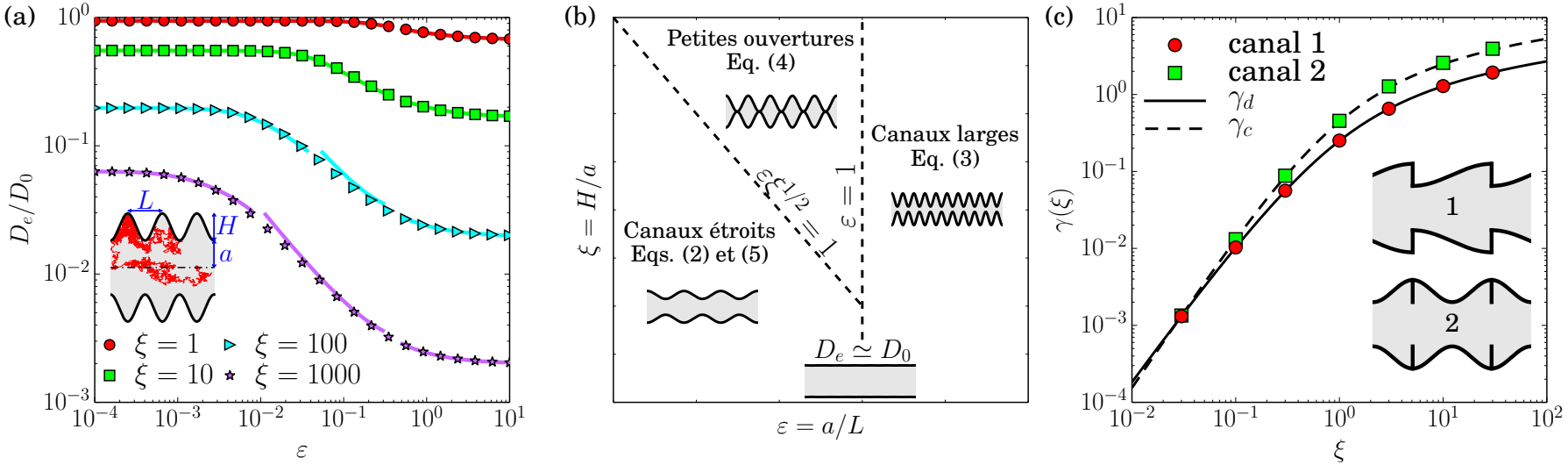

- Characterize the spreading of a cloud of particles initially close.
- The Boltzmann distribution is not reached for these systems.
- The stationary state is described by effective diffusivity D_e.
- We have studied the dispersion in periodic channels, linking it with the geometry.
- We have identified three regimes of dispersion (slowly varying channels, narrow escape, large channels) [Figs. (a-b)], and derived a corresponding expression for D_e.
- We have also looked at the dispersion in discontinuous channels [Fig. (c)].

M. Mangeat, T. Guérin, and D. S. Dean, EPL **118**, 40004 (2017).
M. Mangeat, T. Guérin, and D. S. Dean, J. Stat. Mech. (2017) 123205.
M. Mangeat, T. Guérin, and D. S. Dean, J. Chem. Phys. **149**, 124105 (2018).

Dispersion in complex media (2/2)

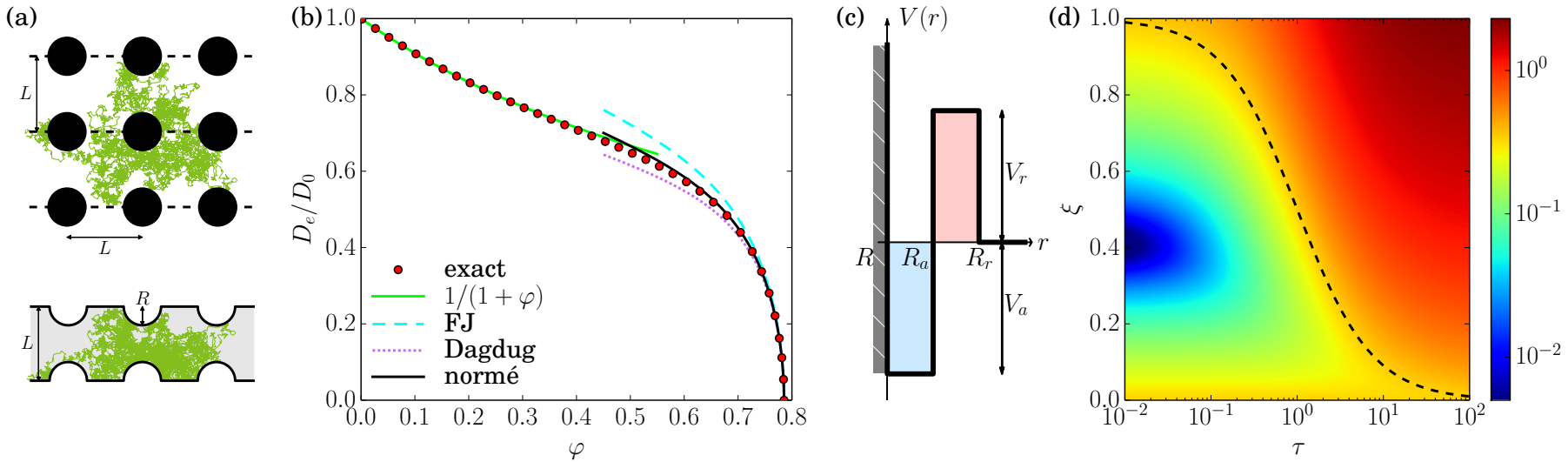

- We have studied the dispersion in obstacle parks, similar to channels [Fig. (a)].
- The effective diffusivity is well characterized in two regimes [Fig. (b)].
- We have also analysed the dispersion for sticky obstacles, with the potential of [Fig. (c)].
- The dispersion can be optimized [below the line of Fig. (d)], for an attractive potential. $\xi = \alpha_a \exp(\beta V_a)$ and $\tau = \alpha_a \alpha_r \exp[\beta(V_a + V_r)]$
- Coupling entropic confinement with energetic confinement can increase the dispersion.

M. Mangeat, T. Guérin, and D. S. Dean, J. Chem. Phys. **152**, 234109 (2020).

Brownian vortexes created by optical traps

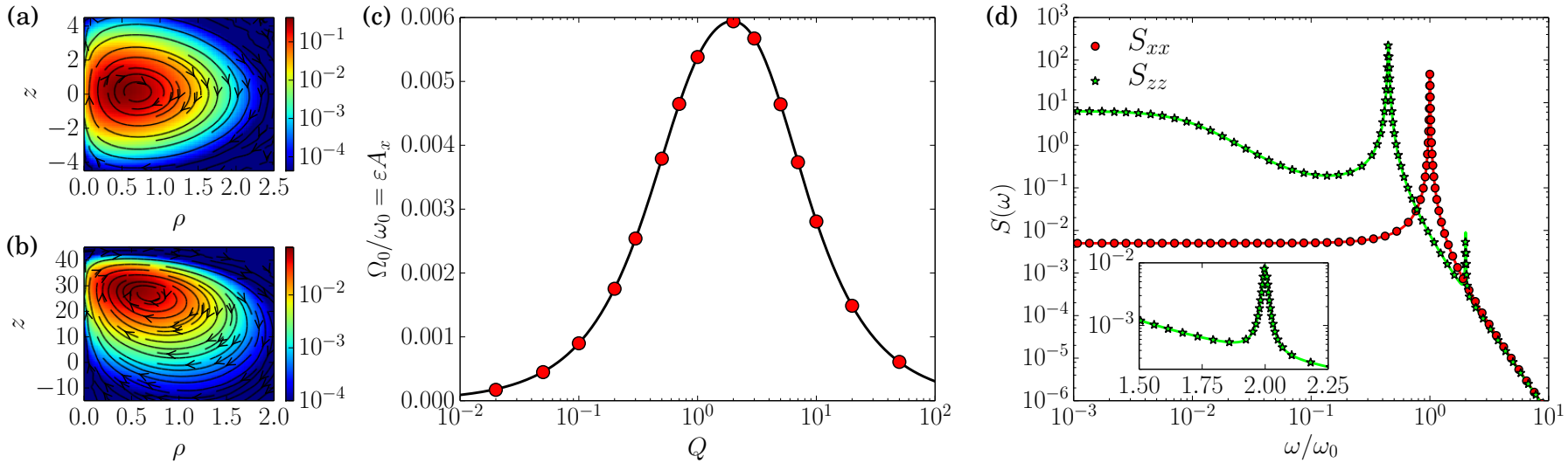

- The radiation pressure of the laser creates a non-conservative force.
- Stationary currents are present and form the Brownian vortexes.
- We looked at the underdamped regime, reached in experiments at low pressure.
- We have calculated the probability density and current [Figs. (a-b)].
- The circulation of the current can be maximized with the damping Q [Fig. (c)].
- We have derived an expression for the power spectrum density [Fig. (d)].

Y. Amarouchene, M. Mangeat, B. Vidal Montes, L. Ondic, T. Guérin, D. S. Dean, and Y. Louyer, Phys. Rev. Lett. **122**, 183901 (2019).

M. Mangeat, Y. Amarouchene, Y. Louyer, T. Guérin, and D. S. Dean, 052107 (2019).

Escape time and cytoskeleton organisation

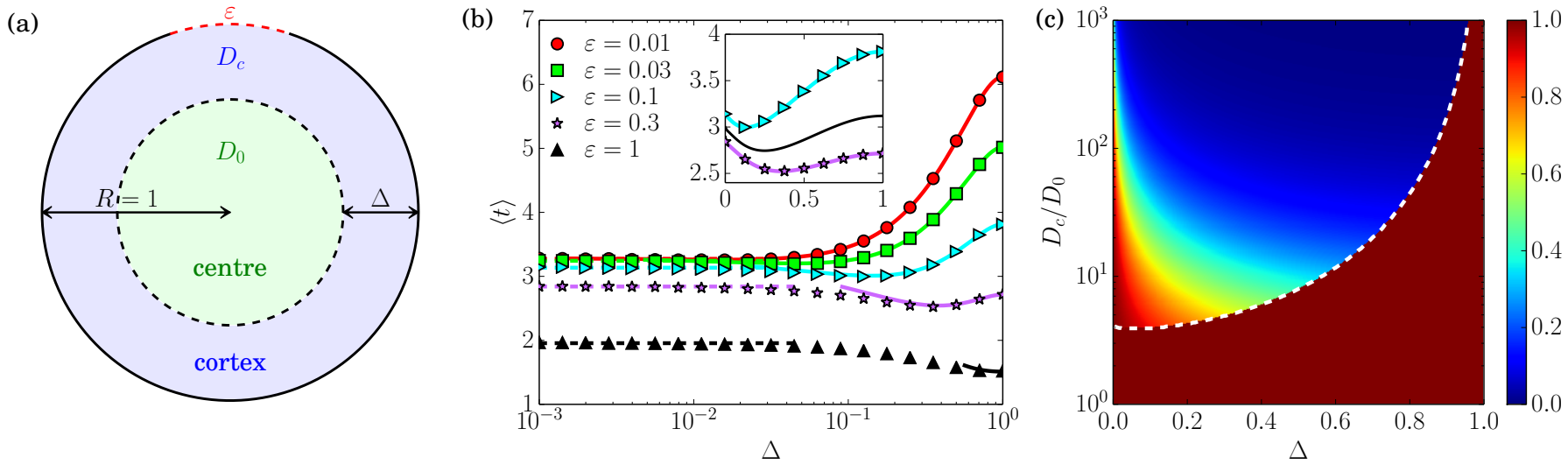

- Intracellular transport of cargo particles through the immunological synapse is crucial for the living cells.
- Time of this transport can be minimized with the size of the actin cortex Δ.
- We have studied a minimal model with just a heterogeneous diffusivity [Fig. (a)].
- The escape time is minimized when the central region is impermeable [Fig. (b)].
- But, the escape time is monotonous for the general problem.
- A mechanism forcing the particles towards the cortex is necessary to have a minimum.

M. Mangeat and H. Rieger, J. Phys. A : Math. Theor. **52**, 424002 (2019).

Collective motion for Potts spins

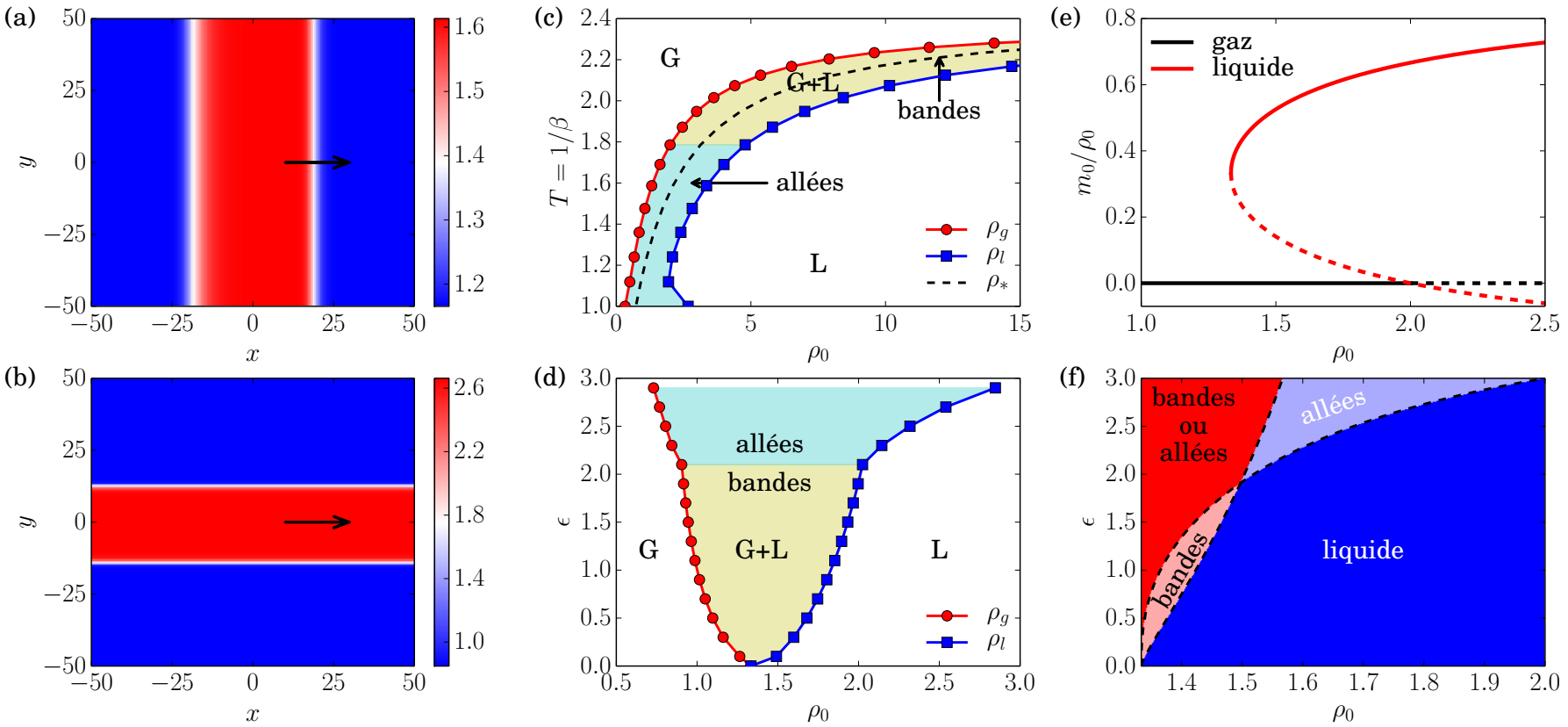

- More details in the second part of the seminar !

S. Chatterjee, M. Mangeat, R. Paul, and H. Rieger, EPL **130**, 66001 (2020)

M. Mangeat, S. Chatterjee, R. Paul, and H. Rieger, Phys. Rev. E **102**, 042601 (2020).

Natural collective motions

Bird flocks :

Ballerini et al., PNAS (2008)

Bacteria swarms :

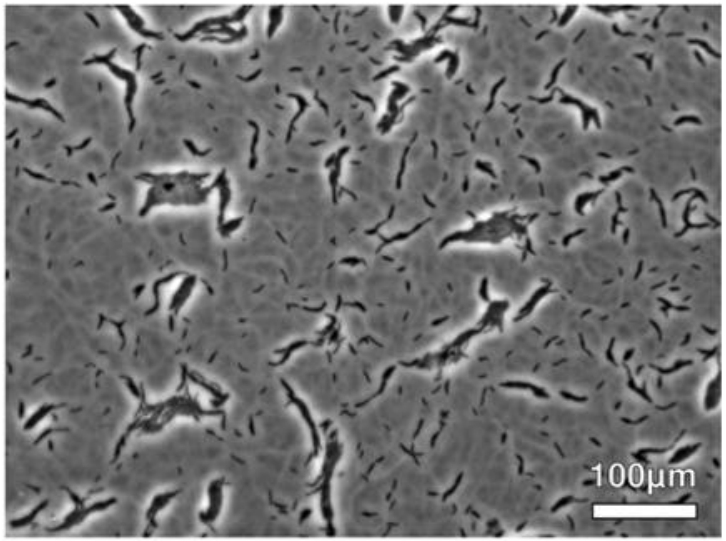

Peruani et al., Phys. Rev. Lett. (2012)

Fish schools :

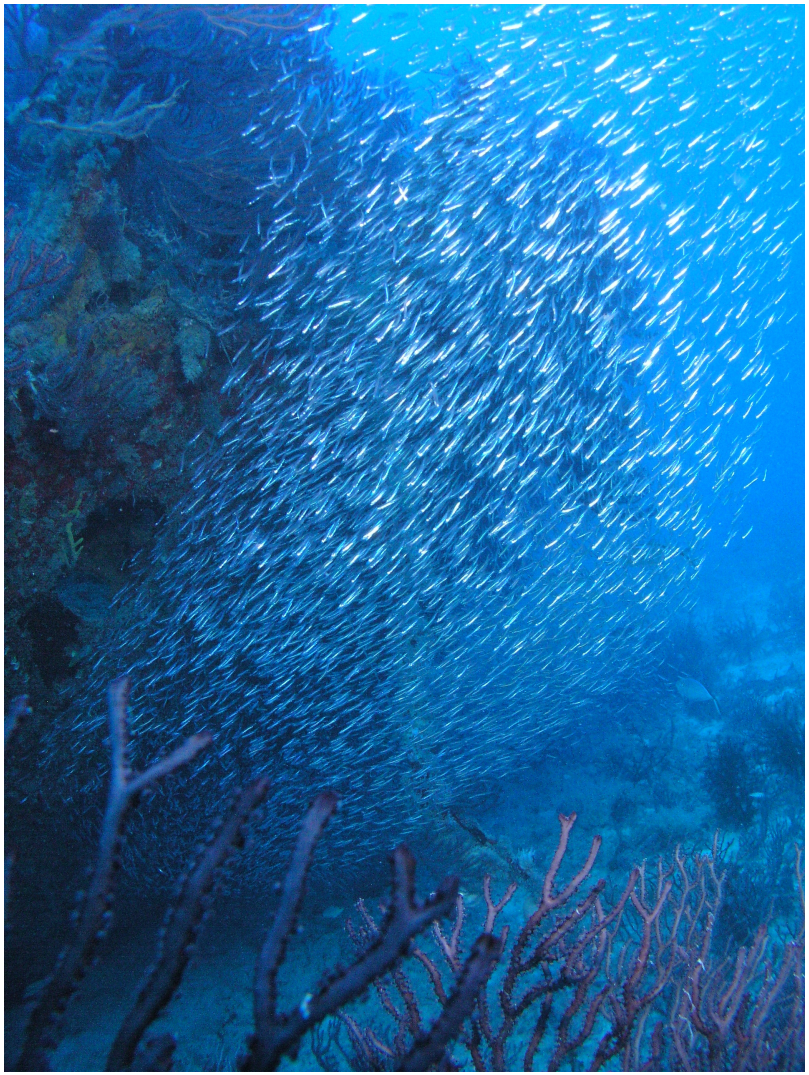

Becco et al., Physica A (2006)

human crowds, molecular motors, ...

Artificial collective motions

Liquid droplets :

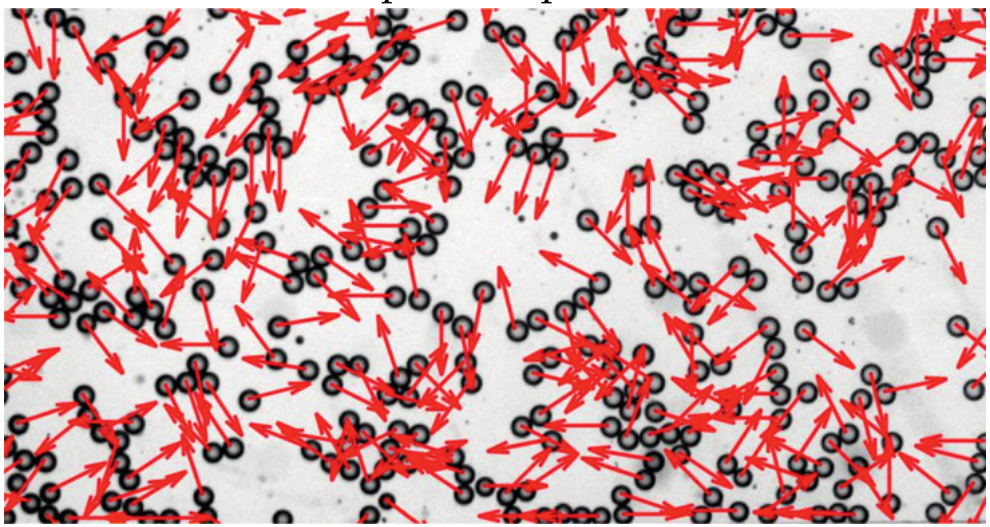

Thutupalli et al., New J. Phys. (2011)

Rolling colloids :

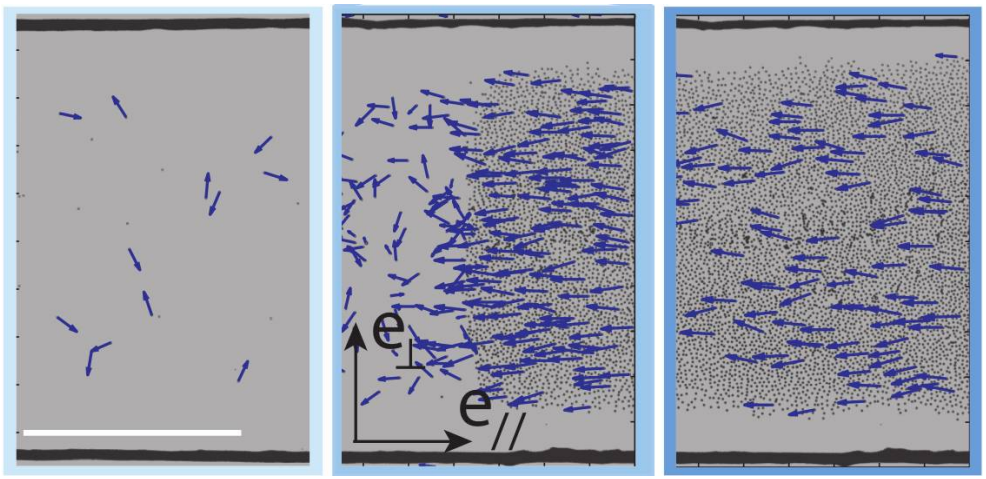

Bricard et al., Nature (2013)

Vibrated polar disks :

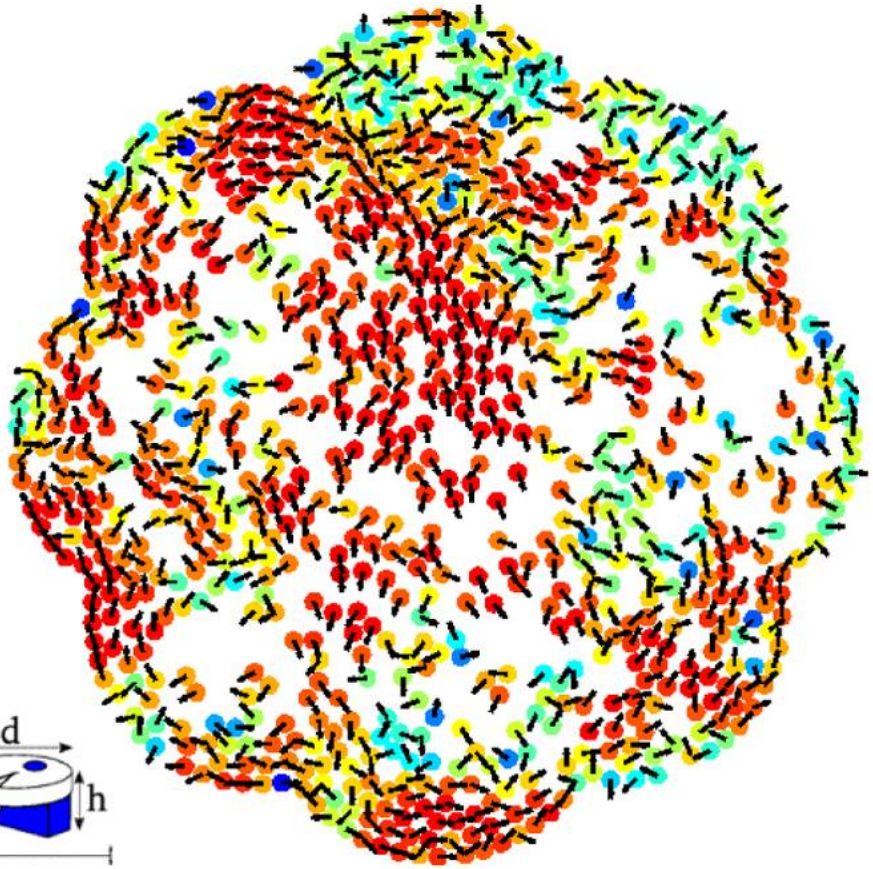

Deseigne et al., Phys. Rev. Lett. (2010)

liquid crystals, ...

How to create a collective motion ?

- Active matter system with a large number of active particles which :
  - consume internal energy to self-propel,
  - interact via alignment and/or repulsion.
- Spontaneous synchronized motion of large clusters emerges for large densities, low noise.
- The clusters are called *flocks*.
- The transition at the emergence of the collective motion is called *flocking transition*.
- It is an out-of-equilibrium phenomenon.

First theoretical model (2D) : The Vicsek model (1995)

- Self-propelled particles with constant speed, aligning in the local average direction.

$$\theta_i(t+dt) = \langle\theta(t)\rangle_r + \eta\xi_i(t)$$
$$\mathbf{x_i}(t+dt) = \mathbf{x_i}(t) + v\mathbf{e_i}(t+dt)dt$$

  with $\mathbf{e_i}(t+dt)$ in the direction of $\theta_i(t+dt)$ and $\xi_i(t)$ a random number in $[-\pi, \pi]$.
- Ferromagnetic interactions where η plays the role of the temperature.

T. Vicsek et al., Phys. Rev. Lett. **75**, 1226 (1995)

- Hydrodynamic limit belongs to universality class of the XY model.

J. Toner and Y. Tu, Phys. Rev. Lett. **75**, 4326 (1995)

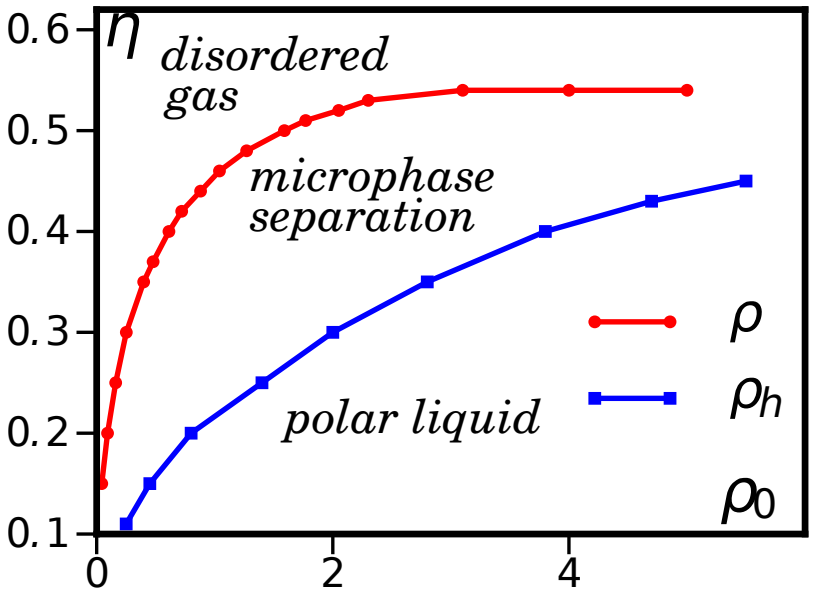

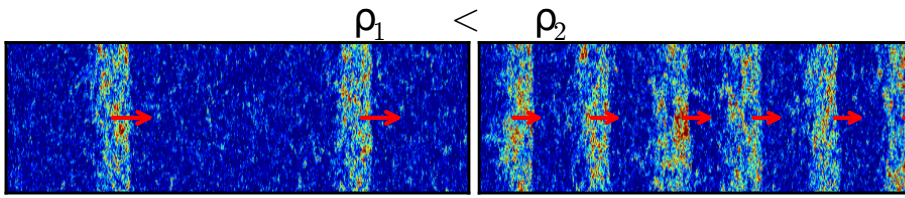

- First-order liquid-gas phase transition, with microphase separation.
- Spontaneous breaking of the continuous symmetry.

A. P. Solon et al., Phys. Rev. Lett. **114**, 068101 (2015)

Active Ising Model (AIM)

Biased Diffusion ***Spin Flips***

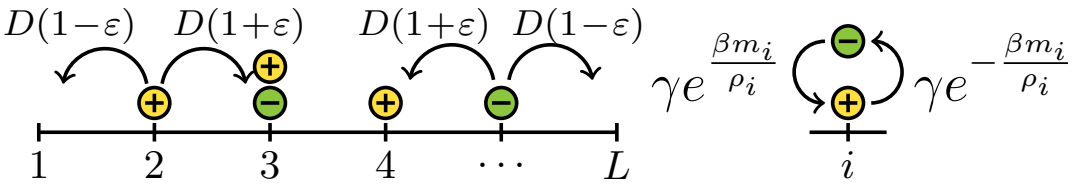

$$W_{\text{hop}} = D(1 \pm \epsilon)$$
$$W_{\text{flip}}(\sigma \to -\sigma) = \gamma \exp(-\beta \sigma m_i / \rho_i)$$

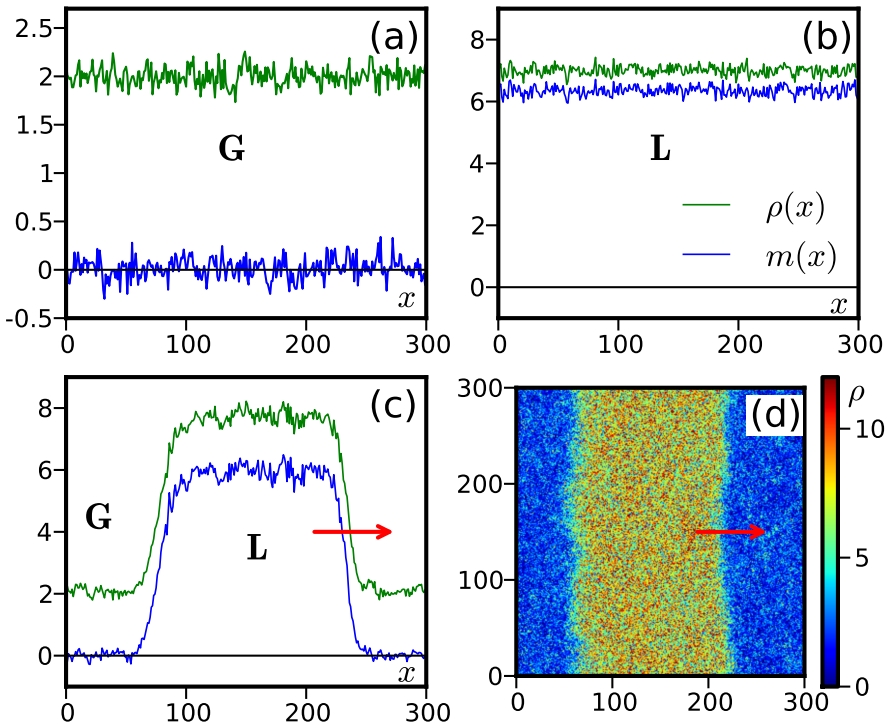

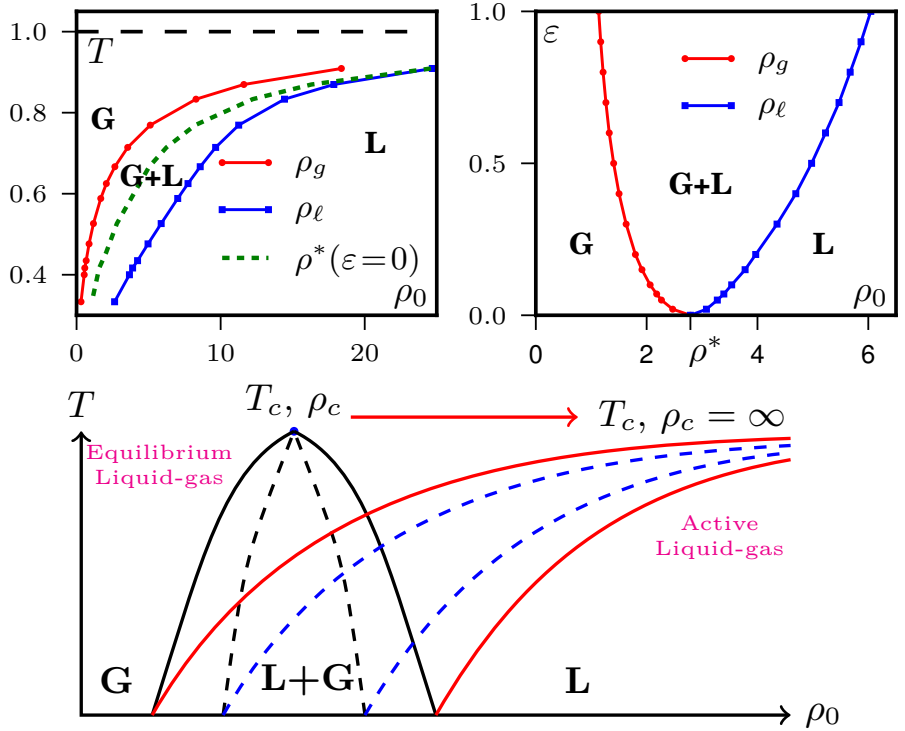

- The flocking transition is a first-order liquid-gas phase transition, without the supercritical region ($T_c = 1$).

A. P. Solon and J. Tailleur, Physical Review E **92**, 042119 (2015)

The microscopic model : generalisation of AIM to q states

- N particles on a periodic lattice with L^2 sites. Average density : $\rho_0 = N/L^2$.
- Spin-state of the kth particle on site i : $\sigma_i^k \in \{1, \dots, q\}$, motion in direction $\phi = \frac{2\pi\sigma_i^k}{q}$.
- $q = 2$: AIM on 1d lattice, $q = 4$: square lattice, $q = 6$: triangular lattice.
- Number of particles in state σ on site i : n_i^σ and local density on site i : $\rho_i = \sum_{\sigma=1}^{q} n_i^\sigma$.

Biased Diffusion

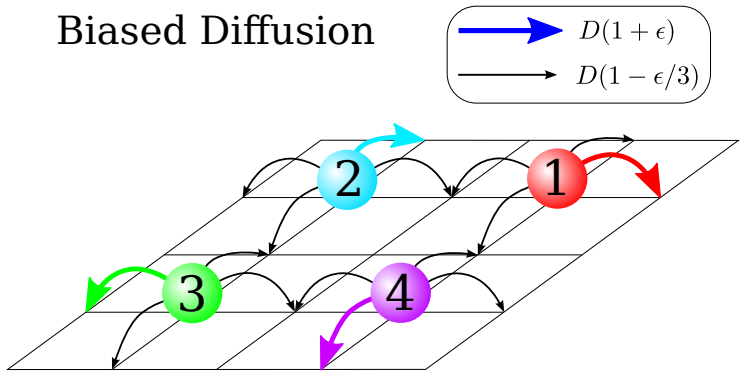

Spin Flips

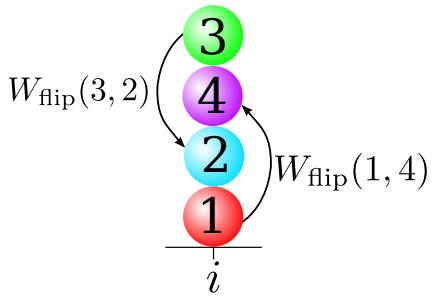

- Hopping rate in preferred direction : $D(1+\epsilon)$ and in other directions : $D\left[1 - \frac{\epsilon}{q-1}\right]$.
- Local magnetisation and local Hamiltonian on site i :

$$m_i^\sigma = \frac{q n_i^\sigma - \rho_i}{q-1}, \qquad H_i = -\frac{J}{2\rho_i} \sum_{k=1}^{\rho_i} \sum_{l \neq k} (q\delta_{\sigma_i^k, \sigma_i^l} - 1).$$

- Flipping rate on site i for a temperature $T = \beta^{-1}$:

$$W_{\text{flip}}(\sigma, \sigma') \propto \exp(-\beta \Delta H_i) = \exp\left[-\frac{q\beta J}{\rho_i}(n_i^\sigma - n_i^{\sigma'} - 1)\right].$$

Microscopic simulations : order-disorder transition at $\epsilon = 0$

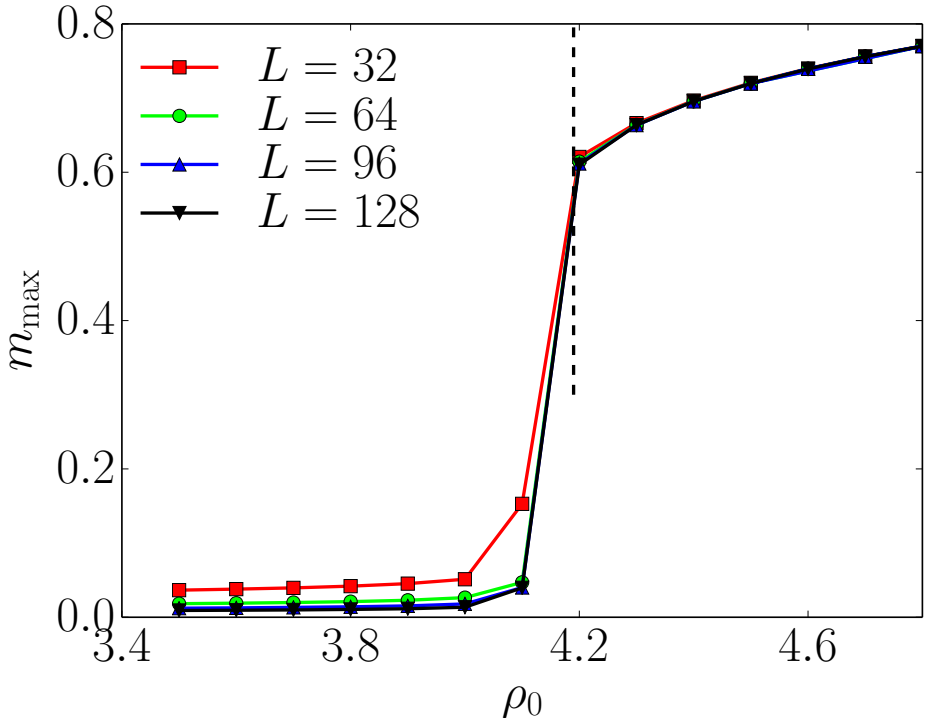

- No phase-separated profiles observed.
- The maximal magnetization $m_{\max} = \max_{\{\sigma\}} \left\langle \frac{m_i^\sigma}{\rho_i} \right\rangle$ is discontinuous.
- First order phase transition at the critical point $\rho_0 = \rho_*$ with a spontaneous breaking of the discrete symmetry Z_4 :
  - $\rho_0 < \rho_*$: disordered phase ($m_{\max} = 0$).
  - $\rho_0 > \rho_*$: ordered phase ($0 < m_{\max} < 1$).

Microscopic simulations : stationary profiles

- Different phases observed ($\epsilon = 0.9$) via density $\rho(x)$ and magnetisation $m(x)$ profiles :

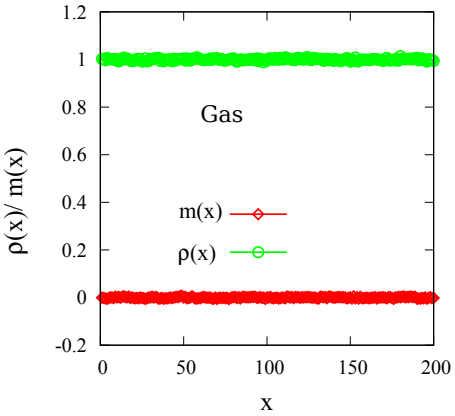

Gas ($\beta = 0.7$, $\rho_0 = 1$)

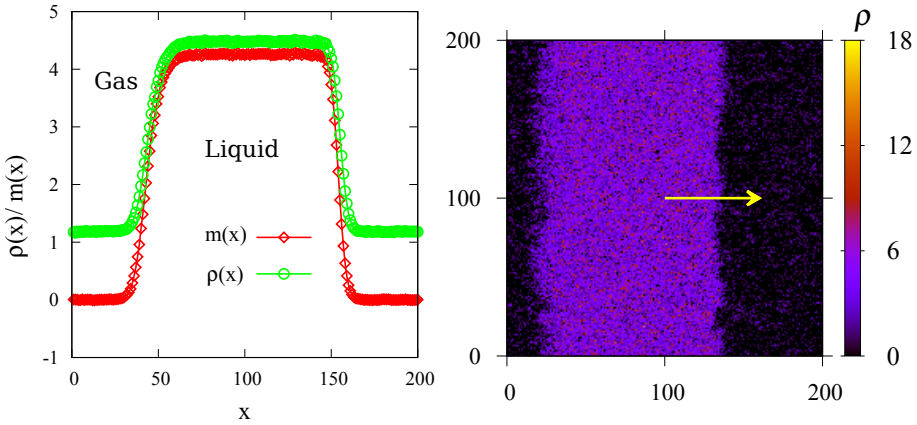

Phase-separation ($\beta = 0.8$, $\rho_0 = 3$)

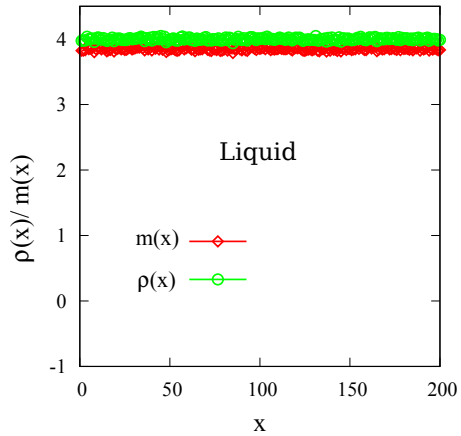

Liquid ($\beta = 0.9$, $\rho_0 = 4$)

- Transverse band motion (small bias) and longitudinal lane formation (large bias) :

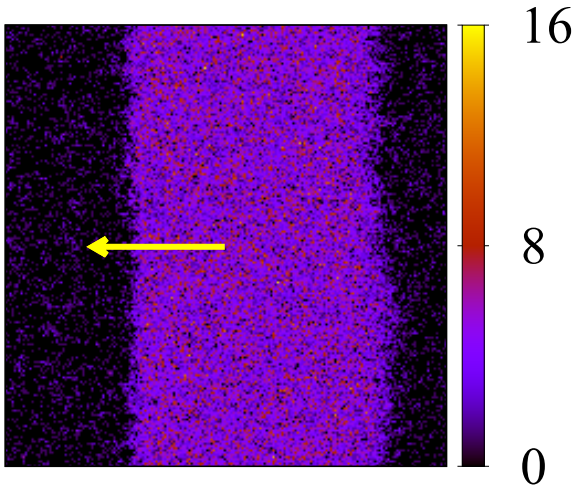

Transverse band ($\epsilon = 0.9$)

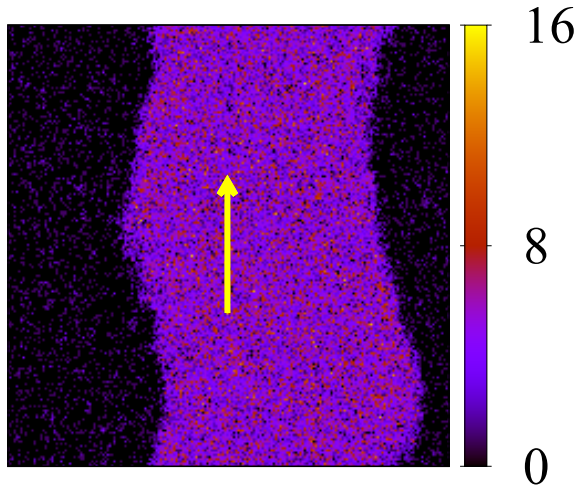

Longitudinal lane ($\epsilon = 1.8$)

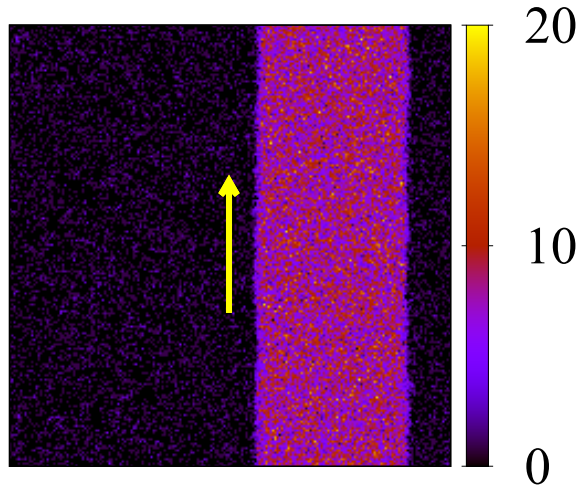

Longitudinal lane ($\epsilon = 2.7$)

Microscopic simulations : phase diagrams

- Phase diagrams : the binodals ρ_g and ρ_l delimit the existence of phase-separated profiles.

(T,ρ_0) diagram for $\epsilon = 2.7$:

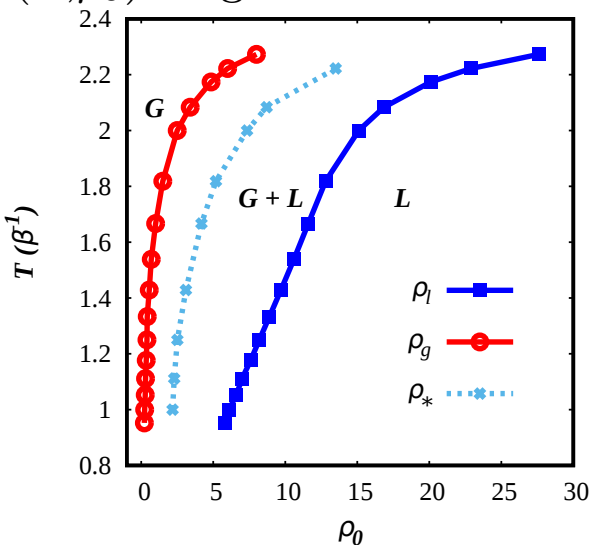

(ϵ,ρ_0) diagram for $\beta = 0.7$:

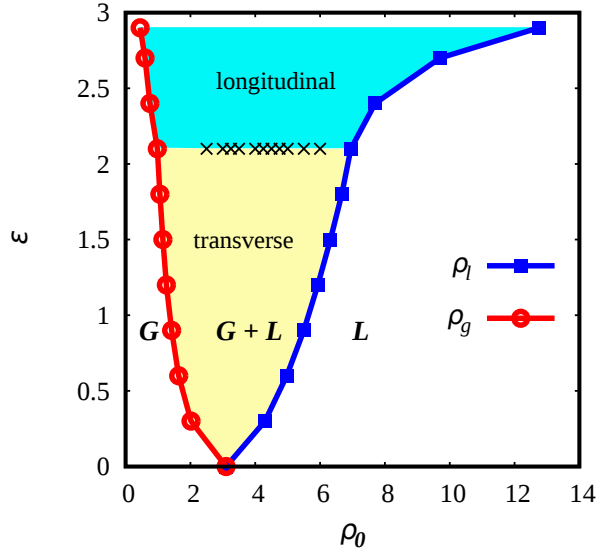

Reorientation transition :

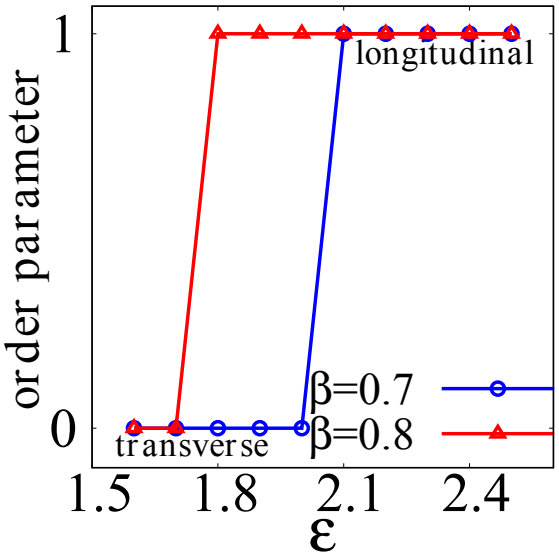

- The flocking transition is a first-order liquid-gas phase transition, similar to VM and AIM , without the supercritical region. Here the critical temperature is $T_c \simeq 2.4$.
- Reorientation order parameter : $\Delta\theta = \langle \cos(\theta - \phi_i) \rangle$ with θ the direction of the stripe.
  - $\Delta\phi = 0$: transverse band.
  - $\Delta\phi = 1$: longitudinal lane.
- The transition bias $\epsilon_*(T)$ is an increasing function of temperature.

From microscopic model to continuum equations

- Hydrodynamic equations for the density of particles $\rho_\sigma(\mathbf{x},t) = \langle n_i^\sigma(t)\rangle$:

$$\partial_t \rho_\sigma = D_\parallel \partial_\parallel^2 \rho_\sigma + D_\perp \partial_\perp^2 \rho_\sigma - v\partial_\parallel \rho_\sigma + \sum_{\sigma' \neq \sigma} \left[\frac{q\beta J}{\rho}(\rho_\sigma + \rho_{\sigma'}) - 1 - \frac{r}{\rho} - \alpha \frac{(\rho_\sigma - \rho_{\sigma'})^2}{\rho^2} \right] (\rho_\sigma - \rho_{\sigma'}),$$

$$D_\parallel = \frac{qD}{4}\left(1 + \frac{\epsilon}{q-1}\right), \qquad D_\perp = \frac{qD}{4}\left(1 - \frac{\epsilon}{q-1}\right), \qquad v = \frac{qD\epsilon}{q-1}$$

- $D_\parallel$ diffusivity in the parallel direction $\mathbf{e}_\parallel = (\cos\phi, \sin\phi)$.
- $D_\perp$ diffusivity in the perpendicular direction $\mathbf{e}_\perp = (-\sin\phi, \cos\phi)$.
- v self-propulsion velocity in the parallel direction $\mathbf{e}_\parallel$.
- Derivatives : $\partial_\parallel = \mathbf{e}_\parallel \cdot \nabla$ and $\partial_\perp = \mathbf{e}_\perp \cdot \nabla$
- $\alpha = \frac{(q\beta J)^2}{2}(1 - 2\beta J/3)$ and r depending on microscopic properties.
- $r = 0$: mean-field equations producing only homogeneous stationary profiles.

Homogeneous solutions for $q = 4$

- Disordered gas : $\rho_\sigma = \rho_0/4$ for a magnetisation $m_0 = 0$.
- Ordered (polar) liquid : $\rho_\sigma = (\rho_0 + 3m_0)/4$ and $\rho_{\sigma' \neq \sigma} = (\rho_0 - m_0)/4$ for a magnetisation

$$\frac{m_0}{\rho_0} = \frac{\beta J}{\alpha}\left\{1 \pm \sqrt{1 + \frac{(\beta - 1 - r/\rho_0)\alpha}{(\beta J)^2}}\right\} \quad \text{when} \quad \begin{cases} \rho_0 > \rho_* = \frac{8(1-2\beta J/3)r}{1+8(2\beta J-1)(1-2\beta J/3)} \\ T < T_c = (1 - \sqrt{22}/8)^{-1} \simeq 2.417 \end{cases}$$

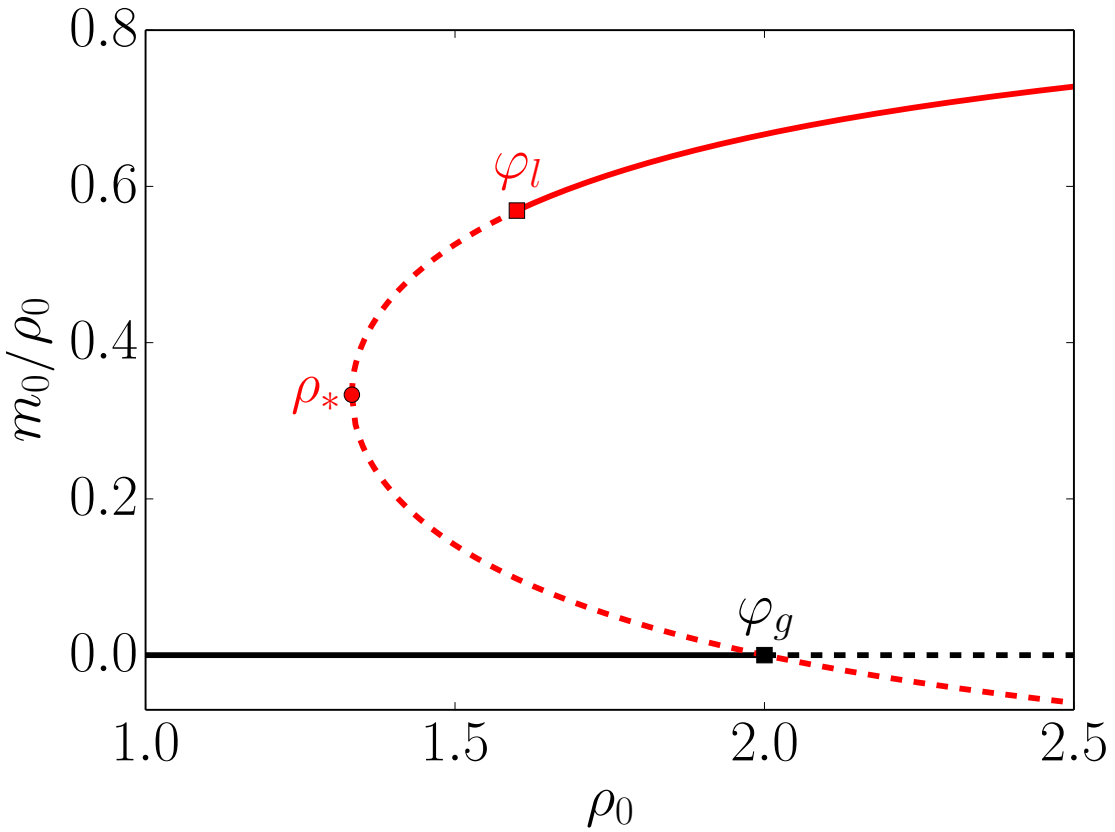

- Transcritical-type bifurcation.
- We recover a first order transition between disordered and ordered phases.

Linear stability analysis for $q = 4$: origin of reorientation transition

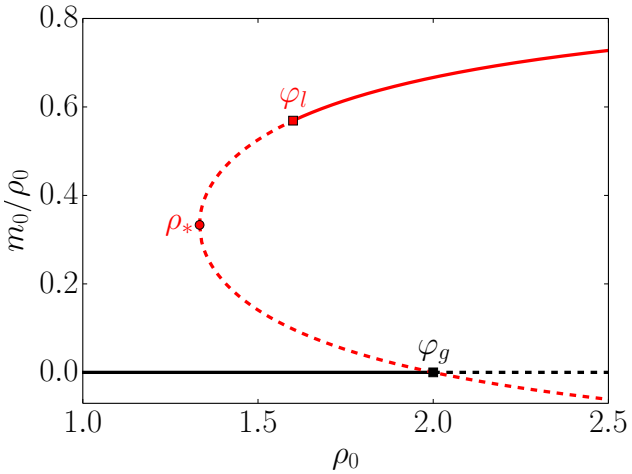

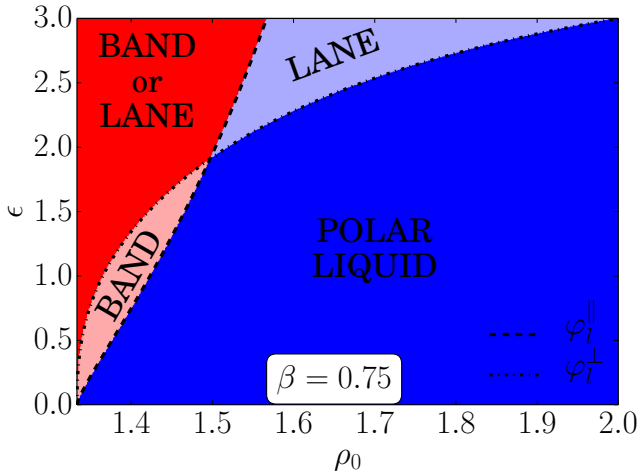

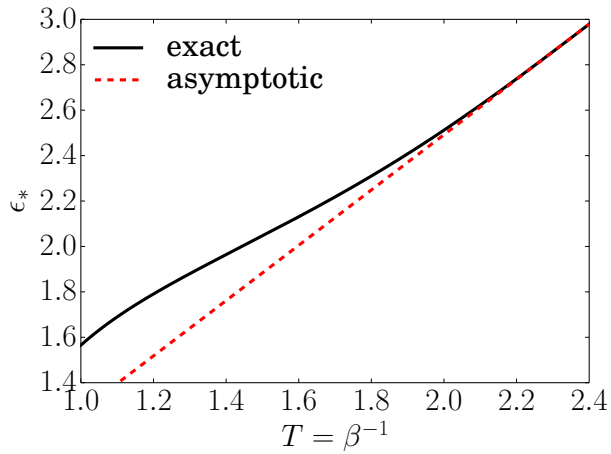

- Effect of small perturbations on homogeneous solutions, leading to spinodals φ_g and φ_l :
  - Gas phase is stable for $\rho_0 < \varphi_g = r/(2\beta J - 1)$.
  - Bands are created for $\rho_* < \rho_0 < \varphi_l^{\parallel}$. ($\lambda_{\parallel} > 0$, perturbation in longitudinal direction)
  - Lanes are created for $\rho_* < \rho_0 < \varphi_l^{\perp}$. ($\lambda_{\perp} > 0$, perturbation in transverse direction)
  - Polar liquid phase stable for $\rho_0 > \varphi_l = \max(\varphi_l^{\perp}, \varphi_l^{\parallel})$. ($\lambda_{\perp} < 0$ and $\lambda_{\parallel} < 0$)
- When $\epsilon = 0$, $\varphi_l = \rho_*$ denotes a first order transition.
- The reorientation transition occurs when $\varphi_l^{\perp} = \varphi_l^{\parallel}$. For $T \to T_c$, the transition velocity is

$$\epsilon_* \simeq 3 \left[1 - 0.981 \frac{T_c - T}{T_c} + \cdots \right].$$

Numerical solutions : density profiles and phase diagrams

- The numerical solutions are obtained with FreeFem++, using the finite element method.
- Transverse band motions and longitudinal lane formations are observed ($\beta = 0.75$) :

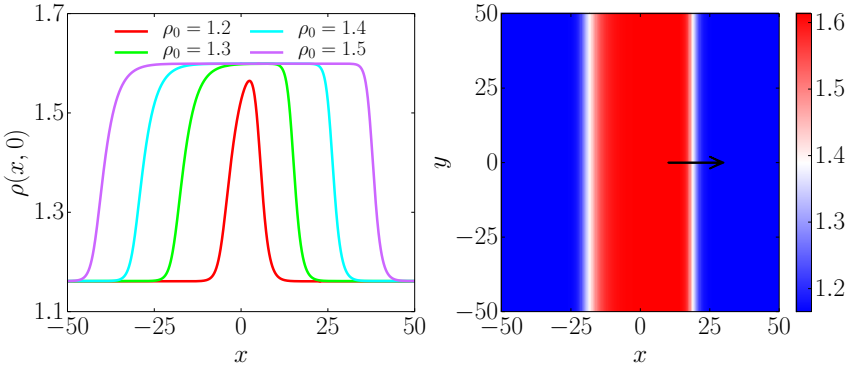

Transverse band ($\epsilon = 0.3$)

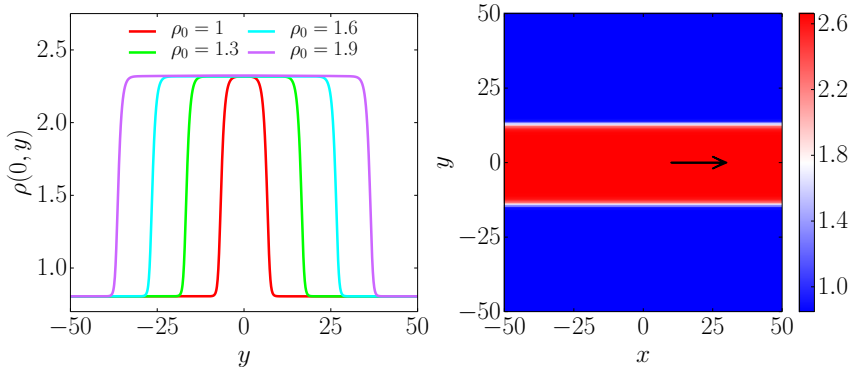

Longitudinal lane ($\epsilon = 2.5$)

- First-order liquid-gas phase transition with critical temperature $T_c \simeq 2.417$.

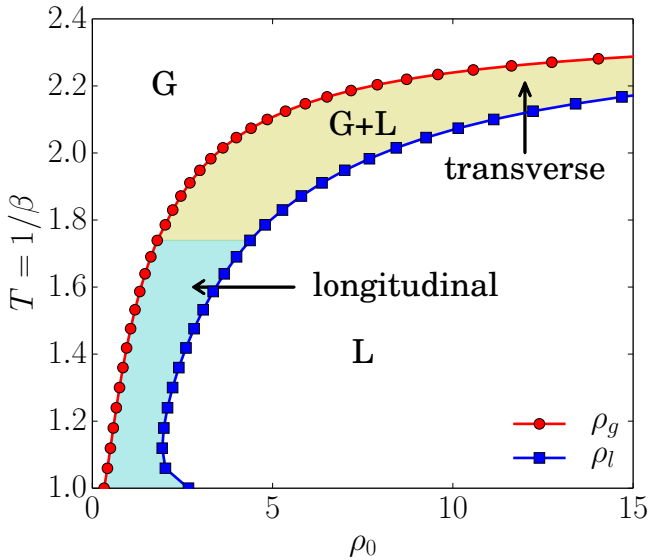

Temperature-density diagram ($\epsilon = 2.5$)

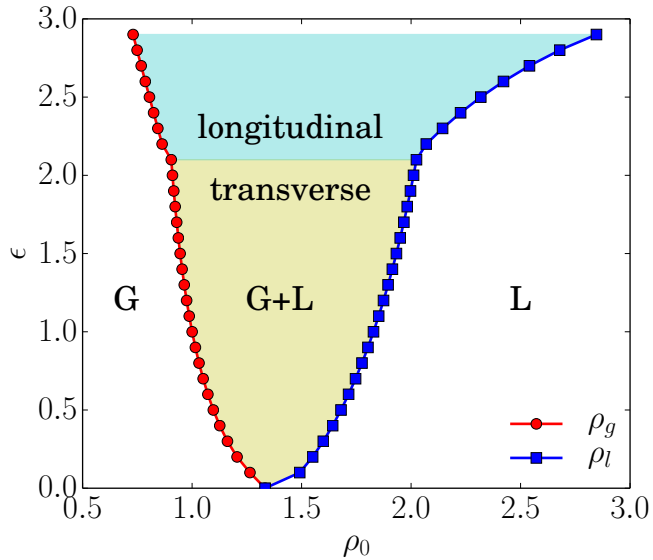

Velocity-density diagram ($\beta = 0.75$)

Conclusion

- The flocking transition is a first-order liquid-gas transition.
- Presence of a reorientation transition between transverse bands and longitudinal lanes.
- Computation of temperature-density and velocity-density phase diagrams.
- Hydrodynamic model reproducing the microscopic simulations.
- Linear stability analysis explaining the origin of the reorientation.

Perspective

- Investigate the $q \to \infty$ limit of the APM.
- Find a model which reproduce the VM in the $q \to \infty$ limit (clock model, XY model ?).
- Introduce a restriction on the maximum number of particles allowed on a single site.

Thank you for your attention !

List of publications :

- S. Chatterjee, M. Mangeat, R. Paul, and H. Rieger, *Flocking and reorientation transition in the 4-state active Potts model*, EPL **130**, 66001 (2020).

- M. Mangeat, S. Chatterjee, R. Paul, and H. Rieger, *Flocking with a q-fold discrete symmetry : Band-to-lane transition in the active Potts model*, Phys. Rev. E **102**, 042601 (2020).

Linear stability analysis

- Eigenvalues obtained with linear stability analysis :

$$\lambda_{\parallel} = \frac{-(D_{\parallel} + 2D_{\perp})\mu + D_{\parallel}\nu}{3\mu - \nu} - \frac{4\mu[-3\mu^2 + 2\mu\nu + \nu(4\kappa + \nu)]v^2}{(3\mu - \nu)^3(3\kappa + \nu)},$$

$$\lambda_{\perp} = \frac{-(2D_{\parallel} + D_{\perp})\mu + D_{\perp}\nu}{3\mu - \nu} + \frac{4\mu v^2}{(3\mu - \nu)(3\kappa + \nu)}.$$

  with $\mu = M(4\beta J - 1 - 2\alpha M + \alpha M^2)$, $\nu = M(4\beta J - 3 + 2\alpha M + 3\alpha M^2)$ and $\kappa = M(-12\beta J + 1 - \alpha M^2)$.

- We can write $M = m_0/\rho_0$ as :

$$M = \frac{\beta J}{\alpha}\left\{1 \pm \sqrt{1 + \frac{(\beta - 1 - r/\rho_0)\alpha}{(\beta J)^2}}\right\} = M_0 \pm M_1\delta.$$

  where $M_0 = \beta J/\alpha$, $M_1 = \sqrt{r/\alpha\rho_*}$ and $\delta = \sqrt{(\rho_0 - \rho_*)/\rho_0}$.

- After some algebraic calculations for $M_1 \ll 1$ $(T \to T_c)$:

$$\epsilon_* = 3\left[1 + \frac{16 + 23M_0}{40M_0(-2 + M_0 + M_0^2)}M_1^2 + \mathcal{O}(M_1^4)\right] = 3\left[1 + \frac{3520 - 993\sqrt{22}}{1160}\frac{T_c - T}{T_c} + \cdots\right].$$